scientific reports

OPEN

Performance of chlorophyll *a* fluorescence parameters in *Lemna minor* under heavy metal stress induced by various concentration of copper

Hanwant Singh, Deepak Kumar & Vineet Soni✉

The objective of the present investigation was to understand the efficacy of chlorophyll fluorescence analysis and to identify the specific photosynthetic parameters for early and rapid detection of Cu-induced HM-stress in plants. Aquatic angiosperm *Lemna minor* was exposed to various concentrations (0–40 μM) of Cu. We observed that the F_V/F_O (Efficiency of the water-splitting complex on the donor side of PSII), quantum yield for electron transport, and quantum yield of primary photochemistry were decreased however, dissipated quantum yield was increased with Cu concentration. ABS/CS_M, TR_O/CS_M, ET_O/CS_M and maximum quantum yield were displayed the dose–response relationship under Cu stress. Performance indexes were increased initially due to the beneficial effects of Cu at lower concentration while decreased significantly ($p \leq 0.05$) at highest concentration of Cu. The outcomes of the present research revealed that the ChlF analysis is very sensitive tool that can be used to determine the toxicity of heavy metals in plants.

In nature, plants are continually exposed to abiotic and biotic stresses. Heavy metals (HMs) like Hg, Cu, Pb, Zn, Ni, Co, Mn, As, etc. have been accumulating in soils for a long time due to anthropogenic activity such as the use of chemical fertiliser, sewage, industrial and smelting wastes[1]. HMs are non-biodegradable elements that cannot be eliminated from the environment through natural processes. Some of them are said to be immobile, that unable to move from the site where they have accumulated, others are referred to as mobile because they can be taken up by the root system of plants via diffusion, endocytosis, or metal transporters[2–13]. However, some metals, such as zinc, copper (Cu), nickel, etc. are important micronutrients that must be absorbed in small amounts as cofactors for several enzymes. Besides these, some HMs found in pesticides such as Cd, Pb, Hg etc. have no beneficial properties and become harmful when their concentration exceeds a threshold limit[14–18]. These HMs may or may not be essential for the proper growth of plants but accumulate in the plants (as a natural accumulator) from soil and water[19–21]. Metal accumulation rates and plant tolerance vary from species to species[22]. Some of the HMs become more toxic than others causing chlorosis, stunted growth, root browning, and mortality are some of the apparent indicators of HM toxicity in plants[23, 24].

Cu (Cu) is an important element in plants that serves several functions at the physiological and molecular levels. However, the excessive levels of it might constitute a risk to the survival of plants. Cu is a key component of plastocyanin and cytochrome oxidase that are essential for photosynthesis and respiration which have a crucial function in plant carbon assimilation and ATP generation[25, 26] Cu-stressed plants exhibit a variety of visible symptoms, including chlorosis, stunted development, ion leakage and reduced root growth[27]. Excessive levels of Cu in plants can lead to oxidative stress that causes severe damage to membranes and macromolecules, as well as having a negative impact on many metabolic pathways[28]. Neelima and Reddy investigated the effects of Cu in *Solanum melongena* seeds and revealed that excess Cu reduces germination, seedling length, and root number[29]. All these consequences are extremely harmful to the plant.

Chlorophyll *a* fluorescence (ChlF) is a commonly used method to detect plant stress conditions in plant research, frequently in association with other morphological, chemical, and physiological variables[30–40]. Chl *a* fluorescence (ChlF) is the natural phenomenon describing the dissipation and heat radiation or re-emission of

Plant Bioenergetics and Biotechnology Laboratory, Department of Botany, Mohanlal Sukhadia University, Udaipur, Rajasthan 313001, India. ✉email: vineetpbbl154@gmail.com

the portion of absorbed energy which is not utilised to drive photosynthesis[23, 41–46]. ChlF measurement provides information about changes in photosynthetic efficiency and heat dissipation[47, 48]. It is an incredibly simple, non-invasive, extremely sensitive, rapid, and accurate method and providing a quantitative assessment of oxygenic photosynthesis[37]. Plants exposed to HM ions disrupt photosynthesis as a result of a single or cumulative event of HM interaction with protein which increase the rate of ROS generation and which replaces essential kations in protein active centers[28].

Some HM ions, for example, Cu, Hg, Cd, Zn, or Ni can replace the core Mg ion in chlorophyll molecules, resulting in chlorophyll-metal complexes and a reduction in PSII quantum efficiency[49–51]. Apart from evaluating specific parameters, of which the F_V/F_O and F_V/F_M are the most well-known and extensively utilised, the interpretation of double normalised curves using the JIP test is becoming increasingly popular in environmental research practices[42]. Plots are formed using data collected at a high sampling rate within a second of the dark-adapted leaf being exposed to light, as the independent variable on a logarithmic timeline. On such plots, inflection points (J-I-P) are noticed when the recorded fluorescence increases which provide the foundation for inferences regarding the photosynthetic apparatus' structure and function. the O-J-I-P transient is prime source of observed variations in the efficiency of the chlorophyll antenna in capturing light energy and transfer to plastoquinone Q_A (the electron acceptor) is the only limitation of photochemical conversion in PSII[52, 53]. Even though, ChlF there are years of in-depth expertise, valid interpretations of ChlF data still require more research[54]. ChlF measurement has become a simple, effective, and dependable technique for outdoor environmental research to improve knowledge and current technology[42, 43, 45, 55–59].

HM, pollution is becoming more prevalent in the environment, demanding rapid and effective solutions for metal remediation. The use of metal-accumulating plants for remediation has recently given rise to a new technology known as phytoremediation[60]. An ideal hyperaccumulator plant species must meet two requirements for this technology to be viable are HM tolerance and accumulation. Consequently, a better knowledge of the metal tolerance mechanism(s) is critical for the development of effective phytoremediation techniques[61]. The chlorophyll *a* fluorescence has long been used to measure the effects of environmental stress on plants, because they provide a quick approach to determine injury in the absence of visual signs[62, 63]. Therefore, the ability to identify the toxic effects before any morphological symptoms can be seen makes phytoremediation an extremely effective method for identifying metal-tolerant plants.

Duckweeds have high potential to grow under HM stress because of their potential to bioremeidte HMs through either by rhizofilteration or phytotransformation. Therefore, besides use in bioremediations, duckweeds serve a rich source of essential HMs such Cu and Zn for improving feed efficiency of animals[64].

Chlorophyll (Chl) *a* fluorescence signals have become one of the potent indicators for early detection of HMs in soil and aquatic bodies[25, 65, 66]. In the present study, we used the chlorophyll (Chl) *a* fluorescence transient to investigate the effects of HM stress induced by various concentration of Cu in *L. minor* plants grown in a nutrient medium.

Materials and methods

Plant material and growth condition. *L. minor* plants were collected from the region of Ayad river located at Udaipur, India (24° 35′ 14.97″ N, 73° 42′ 38.75″ E) (As per the Biological Diversity act, 2002 of National Biodiversity Authority of India, the Indian researchers neither require prior approval nor need to give prior intimation to SBB for obtaining biological resource for conducting research[67]). The plant was identified by Dr. Vineet Soni based on the morphological characteristics (oval shaped fronds, 2–5 fronds remained together, presence of three nerves in each frond and cylindrical root sheath with two lateral wings). The collected fronds (stock culture) were maintained in plastic (PVC) aquariums in Jacob culture media as per the OECD guideline of 2002[68]. The stock culture and Cu treated plants were kept in controlled conditions at 150–230 μmol/m²/s (PAR) by using white fluorescent light, 14:10 h light: dark cycle, and 25/20 °C day/night temperature. This medium consisted of the following: Stock solution (A): Ca (NO$_3$)$_2$, 60.0 g/L, Stock solution (B): MgSO4·7H$_2$O, 102.0 g/L; KNO$_3$, 100.0 g/L; KH$_2$PO$_4$, 14.0 g/L, Stock solution (C): H$_3$BO$_4$, 0.300 g/L; MnCl$_2$·4H$_2$O, 0.3145 g/L; ZnSO$_4$·7H$_2$O, 0.0356 g/L; Na$_2$MoO$_4$·2H$_2$O, 0.0118 g/L, Stock solution (D): CuSO$_4$·5H$_2$O, 0.0125 g/L; FeEDTA (Ethylenediaminetetraacetate acid), 1.8520 g/L. Stock solutions were kept in a refrigerator and growth media prepared by adding 10 mL of each stock to 1 L of distilled water and then adjusting the pH 6.0 using NaOH or HCl[69].

Cu exposure. For the ChlF experiment ~ 30 two or three-fronded, healthy plants (300 mg) were taken from stock culture and transferred to glass bottle containing 250 mL of growth medium without EDTA and exposed to various concentrations of CuSO$_4$·5 H$_2$O (Sigma Aldrich, C8027, ≥ 98%) (0, 10, 20, 30, and 40 μM) for 24 h. The metal exposure experiments were performed according to procedure described by Teisseire and Guy using EDTA free growth medium since it is a chelating agent and alter the metal adsorption process in plants (can increase the bioavailability of metal)[70]. Control plants were grown under both EDTA and Cu free growth medium. The experiment glass bottles were placed in a controlled environment as described above.

Chlorophyll a fluorescence transient. ChlF was measured using a plant efficiency analyser (Handy PEA fluorimeter, Hansatech instruments Ltd. England). Before measurement fronds were dark-adapted for 50–60 min at 26 °C. Thereafter, ChlF signals were analysed with the Biolyzer v.3.0.6 software (developed by Laboratory of Bioenergetics, University of Geneva, Switzerland). The experiments were done in six replicates and repeated three times to ensure the results. JIP-test method has been developed by which several selected phenomenological and biophysical parameters quantifying the PSII and PSI behaviors are calculated. Several parameters can be derived from the polyphasic ChlF rise (OJIP curve) that provide information about photo-

Parameters	Coefficients of PC1	Coefficients of PC2
Tf(max)	− 0.14954	− 0.37572
Area	0.22914	− 0.19298
Fo	0.16258	0.39279
Fv	0.24298	0.11948
Fm	− 0.251	− 0.0207
Vj	0.24927	0.02706
Fv/Fo	− 0.24935	0.04374
Vi	− 0.21397	0.20491
N	− 0.24055	− 0.05733
ABS/RC	− 0.23608	0.16507
TRo/RC	− 0.20833	0.27505
ETo/RC	0.16819	0.38453
DIo/RC	− 0.24915	0.05531
ABS/CSo	0.13162	0.44138
TRo/CSo	0.23242	0.19605
ETo/CSo	0.2498	0.05198
DIo/CSo	− 0.24981	0.05349
PI(abs)	0.22676	− 0.22471
PI(csm)	0.23513	− 0.18388

Table 1. Principal component analysis of chlorophyll *a* flourescence parameters of *L. minor* under various concentration of Cu.

synthetic fluxes[41, 71–73]. Abbreviations, formulas, and definitions of the JIP-test parameters used in the current study are presented in Table 1.

Principal component analysis (PCA), grid correlation matrix and heat map. The relations between the selected JIP-test parameters were tested by Principal Component Analysis. ChlF parameter was selected for the PCA analysis to classify the variables that show the maximal fluctuations. Dimension 2 (PC 2) described the maximum of the variability which accounted for 79.15% and dimension 1 (PC 1) accounted for 18.17%, respectively. The positive and negative correlation between the parameters also shows the variation of the parameters in the respective principal components (dimensions) (Table 2). The correlation between all ChlF parameters investigated in this paper were analysed through grid correlation matrix by using Python software which expressed between + 1 and − 1 with colour code. The calculated JIP parameters were also presented by the heat map, through normalizing them between 1 and 100 by using a color code green to red.

Statistical analysis. Statistical analysis was performed using analysis of variance (ANOVA), followed by a Tukey HSD test ($p = 0.05$) using XLSTAT 2020. Only significant values ($p \leq 0.05$) of measurements are presented in figures. The heat map was prepared by normalizing the values and bringing them all to a range between 1 and 100 to provide an unbiased color code. Three color code combination of red for high (100%), yellow for medium (50%), and green for the lowest value (1%) was used to represent the heat map. The MS excel and CorelDraw software were used for calculation and designing of the heatmap. In addition, a principal component analysis (PCA) was conducted by eigenvalue decomposition of a data correlation matrix using OriginPro 2016. PCA was applied to find the patterns of the fluorescence parameter and variations in the experimental data. The 48-h lethal dose (LD_{50} and LD_{90}) was determine by Probit Analysis using SPSS (22.0). Comparision of mortality ratios between experimental and control groups in the deferent concentrations was performed with Chi-square testing.

Results
Cu stress significantly altered the growth and productivity of *L. minor* through the modulation of the photosynthetic process. In the present studies, impacts of Cu-induced HM stress on ChlF kinetics, specific energy fluxes, phenomenological energy fluxes, and performance indexes were studied in *L. minor*.

ChlF rise. ChlF rise of *L. minor* was measured after 24 h of Cu treatment and a typical OJIP induction curve was displayed when plotted on the logarithm time scale (Fig. 1). With increasing the Cu concentration, the fluorescence yield at various intermediary steps, such as J, I, and P was reduced. In control plants, two intermediate peaks F_J (chlorophyll fluorescence at 2 ms) and F_I (chlorophyll fluorescence at 300 ms) were formed between F_O and F_M, ChlF increased continuously from initial (F_O) to maximal (F_M) fluorescence intensity in *L. minor* growing under control conditions. HM induced reduction in PSII photochemistry and electron transport activity were severe at the highest concentration of Cu.

Basic parameters calculated from the extracted data	
$F_O \cong F_{50\mu s}$ or $\cong F_{20\mu s}$	Fluorescence when all PSII RCs are open ($\cong$ to the minimal reliable recorded fluorescence)[81]
$T_{FM} = tF_{MAX}$, t for F_M	Time (in ms) to reach maximal fluorescence F_m[81, 110]
$F_M (= F_P)$	Maximal fluorescence, when all PSII RCs are closed ($= F_P$ when the actinic light intensity is above 500 μmol(photon) m^{-2} s and provided that all RCs are active as Q_A-reducing)[81, 110]
$F_V \equiv F_M - F_O$	Maximal variable fluorescence[81]
$S_M \equiv Area/(F_M - F_O) = Area/F_V$	Normalised Area to F_m[81]
$N = S_M \times (M_O/V_J)$	Turnover number (expresses how many times Q_A is reduced in the time interval from 0 to tF_M)[81]
$V_J = (F_J - F_O)/(F_M - F_O)$	Relative variable fluorescence at t = 2 ms[81]
$V_I = (F_I - F_o)/(F_M - F_o)$	Relative variable fluorescence at t = 30 ms[81]
Biophysical parameters derived from the basic parameters	
Deexcitation rate constants of PSII antenna	
$k_N = (ABS) \times k_F \times (1/F_M)$	Nonphotochemical deexcitation rate constant (ABS: absorption flux—see below; k_F: rate constant for fluorescence emission)[42, 81, 110]
$k_P = (ABS) \times kF \times (1/F_O - 1/F_M) = k_N \times (F_V/F_O)$	Photochemical deexcitation rate constant[81, 110]
Specific energy fluxes (per RC: QA-reducing PSII reaction centre), in ms^{-1}	
$ABS/RC = M_O \times (1/V_J) \times (1/\varphi P_o)$	Absorption flux (exciting PSII antenna Chl a molecules) per RC (also used as a unit-less measure of PSII apparent antenna size)[74, 81, 110]
$TR_O/RC = M_O \times (1/V_J)$	Trapped energy flux (leading to Q_A reduction), per RC[81]
$ET_O/RC = M_O \times (1/V_J) \times (1 - V_J)$	Electron transport flux (further than Q_A^-), per RC[81]
$DI_o/RC = ABS/RC - TR_o/RC$	Dissipated energy flux per RC (at t = 0)[81]
Phenomenological energy fluxes (per CS: QA-reducing PSII cross section), in ms^{-1}	
$TR_O/CS_M = (F_v/F_M)(ABS/CS_M)$	Trapped energy flux (leading to Q_A reduction) per RC[81]
$ET_O/CS_M = (F_v/F_M)(1 - V_J)(ABS/CS_M)$	Electron transport flux (further than Q_A^-) per RC[81]
$DI_O/CS_M = (ABS/CS_O) - (TR_O/CS_m)$	Total energy dissipated per reaction center (RC)[81]
$ABS/CS_M = \approx Fo$	Absorbed photon flux per excited PSII cross section at time zero[81]
Quantum yields and efficiencies	
$\varphi_{Po} \equiv TR_0/ABS = [1 - (F_O/F_M)]$	Maximum quantum yield for primary photochemistry[81]
$\varphi_{Eo} \equiv ET_0/ABS = [1 - (F_O/F_M)] \times (1 - V_J)$	Quantum yield for electron transport (ET)[74]
$\psi_{Eo} \equiv ET_0/TR_0 = (1 - V_J)$	Efficiency/probability that an electron moves further than Q_A^-[74]
$\phi D_o = F_o/F_m$	Quantum yield (at t = 0) of energy dissipation[74]
Performance indexes	
$PI_{ABS} = \frac{1-(F_O/F_m)}{M_O/V_j} \times \frac{F_m/F_o}{F_O} \times \frac{1-V_j}{V_j}$	Performance index for energy conservation from photons absorbed by PSII until the reduction of intersystem electron acceptors[74, 81, 110]
$PI_{CS} = \frac{ABS}{CS} \times \frac{1-(F_O/F_m)}{M_O/V_j} \times \frac{F_m/F_o}{F_O} \times \frac{1-V_j}{V_j}$	Performance index on cross section basis[74, 81, 110]

Table 2. Abbreviations, formulas, and definitions of the JIP-test parameters.

Biophysical parameters derived by the 'JIP-test' equations'. F_O and F_M. The minimal fluorescence intensity (F_O) and the maximum fluorescence intensity (F_M) both are decreased with increasing the Cu concentration (Fig. 2A). Fluorescence intensity recorded at 50 μs is denoted as F_O and at this time the all primary quinone acceptor (Q_A) is in the open (oxidized) state.

The maximum primary yield of photochemistry of PS I1 (F_V/F_O) are related with photosynthetic efficiency of plant and increased value of F_V/F_O indicates proper functioning of PSII. The F_V/F_O ratio (ratio between the rate constants of photochemical and nonphotochemical deactivation of excited Chl molecules) for *L. minor* plants decreased gradually at 10 μM (94.86% of control) and 30 μM (89.44% of control) concentration of Cu (Fig. 2A). Further, a significant decline in F_V/F_O ratio (43.58% of control) was recorded at a high level (40 μM) of Cu exposure as a result of a significant decrease in F_V (41.00% of control) as shown in Figs. 2A and 3.

The relative variable fluorescence at 2 ms (J step) is denoted as V_J which is the measure of the fraction of primary quinone electron acceptor of PSII in its reduced state [$Q_A - /Q_{A(total)}$][74]. At the lower level of HM stress, a slight reduction in the value of V_J was observed but with increasing the metal concentration to a high level the V_J value was increased to 224.74% of control (Figs. 2A, 3).

Complimentary Area (S_M) is also an important parameter that is directly proportional to the number of reduction and oxidation of one Q_A^- molecule during the fast OJIP transient or number of electrons passing through the electron transport chain[75]. The turnover number (N) is represented as the number of times Q_A becomes reduced and re-oxidized another time, till the F_M (Maximum fluorescence intensity) is reached[76–79]. At severe Cu stress the increased value of turnover number (N) value was recorded (145.40% of control) which was also represented by PSI cyclic electron transport as photoprotection (Fig. 2A). The increased values of S_M in *L. minor*
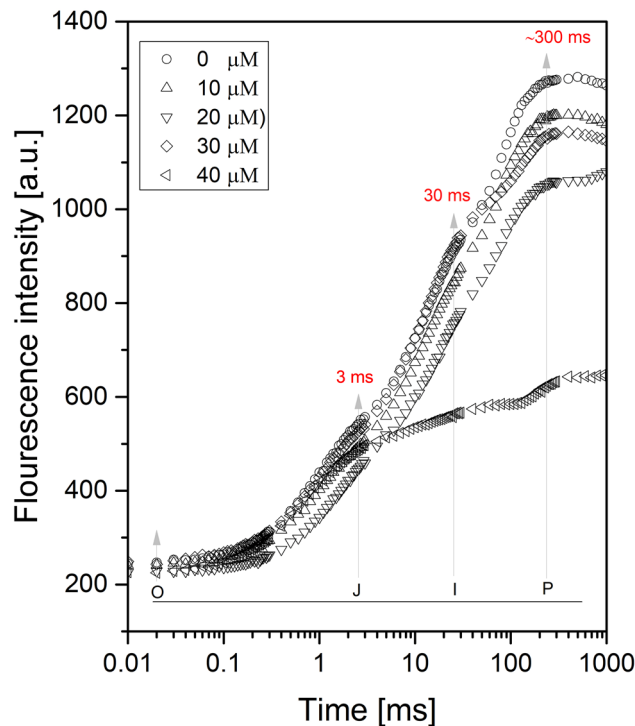
Figure 1. ChlF rises in *L. minor* plants exposed 24 h. to different concentrations of $CuSO_4$ (0.0 μM to 40.0 μM) and O, J, I, and P indicate PSII rapid fluorescence transients.

under Cu exposure (131.40% of control at moderate HM treatment) displayed the reduced electron transport between these photosystems.

Quantum yield. The quantum yield of primary photochemistry F_V/F_M (φPo), which reflects the overall photosynthetic potential of active PSII reaction centers, was not affected by Cu-induced HM stress in plants. However, a slight decline in F_V/F_M was recorded at 40 μM Cu (Fig. 2C). A similar trend was observed in ET/ABS (φEo) (Figs. 2C, 3). The lowest values of φEo, approximately half of control, were recorded when *L. minor* was subjected to 40 μM Cu. In contrast, DI/ABS (φDo) remained almost the same until the exposure of 30 μM Cu and thereafter enhanced about two folds of the control level in plants grown in media containing 40 μM Cu (Figs. 2C, 3).

Specific energy flux (membrane model). The specific energy fluxes such as absorption flux per reaction center (ABS/RC), trapped energy flux per reaction center (TR_O/RC), electron transport flux per reaction center (ET_O/RC), and dissipated energy flux per reaction center (DI_O/RC) were analyzed to determine the photosynthetic performance of active PS II reaction centers of *L. minor* subjected to various concentrations of Cu (Figs. 3, 4). Up to 30 μM Cu, no significant variations in absorption flux per reaction center (ABS/RC) was recorded while at 40 μM, a remarkable enhancement in absorption potential of active reaction centers was recorded (162.83% of control) (Figs. 3, 4). A similar trend in TR_O/RC was observed as shown in the heatmap (Fig. 3). TR_O/RC remained almost constant up to 30 μM Cu and thereafter increased with increasing the severity of Cu-induced HM stress (129.68% of control). In contrast, no significant changes in electron transport flux per reaction center (ET_O/RC) were recorded up to 20 μM Cu concentration while decreased at severe Cu stress (73.58% of control). On the contrary, the DI_O/RC remained constant up to 30 μM Cu and then increased about three folds with the progression of Cu concentration (297.67% of control) as shown in Fig. 2B. The effects of Cu-induced HM stress on the specific energy fluxes (absorption flux per reaction center, trapped energy flux per reaction center, electron transport flux per reaction center, and dissipated energy flux per reaction center) are presented diagrammatically through thylakoid membrane models (Fig. 4). It is of interest to investigate if HM stress changes the ratio among antenna light-harvesting complex (ABS) and active PSII reaction centers (RC). According to the leaf pipeline model in severe Cu stress, there is more active RC and the higher value of specific energy flux (ABS/RC, TR_O/RC, and DI_O/RC) shows the increased ability of RC to the reduction of plastoquinone (Fig. 4).

Phenomenological energy flux (leaf model). Phenomenological energy fluxes mean absorption flux per cross-section (ABS/CS), trapped energy flux per cross-section (TR_O/CS_M), electron transport flux per cross-section (ET/CS), and dissipated energy flux per cross-section (DI_O/CS_M) significantly modulated by Cu-induced HM stress in *L. minor*. Absorption flux per cross-section (ABS/CS_M) did not alter with increasing concentrations of Cu up to 30 μM (Fig. 5). The lowest values of ABS/CS_M, TR_O/CS_M and ET_O/CS_M were noticed at the highest concentration of Cu (92.09%, 73.34% and 41.61% of control respectively). Absorption potential per cross-section
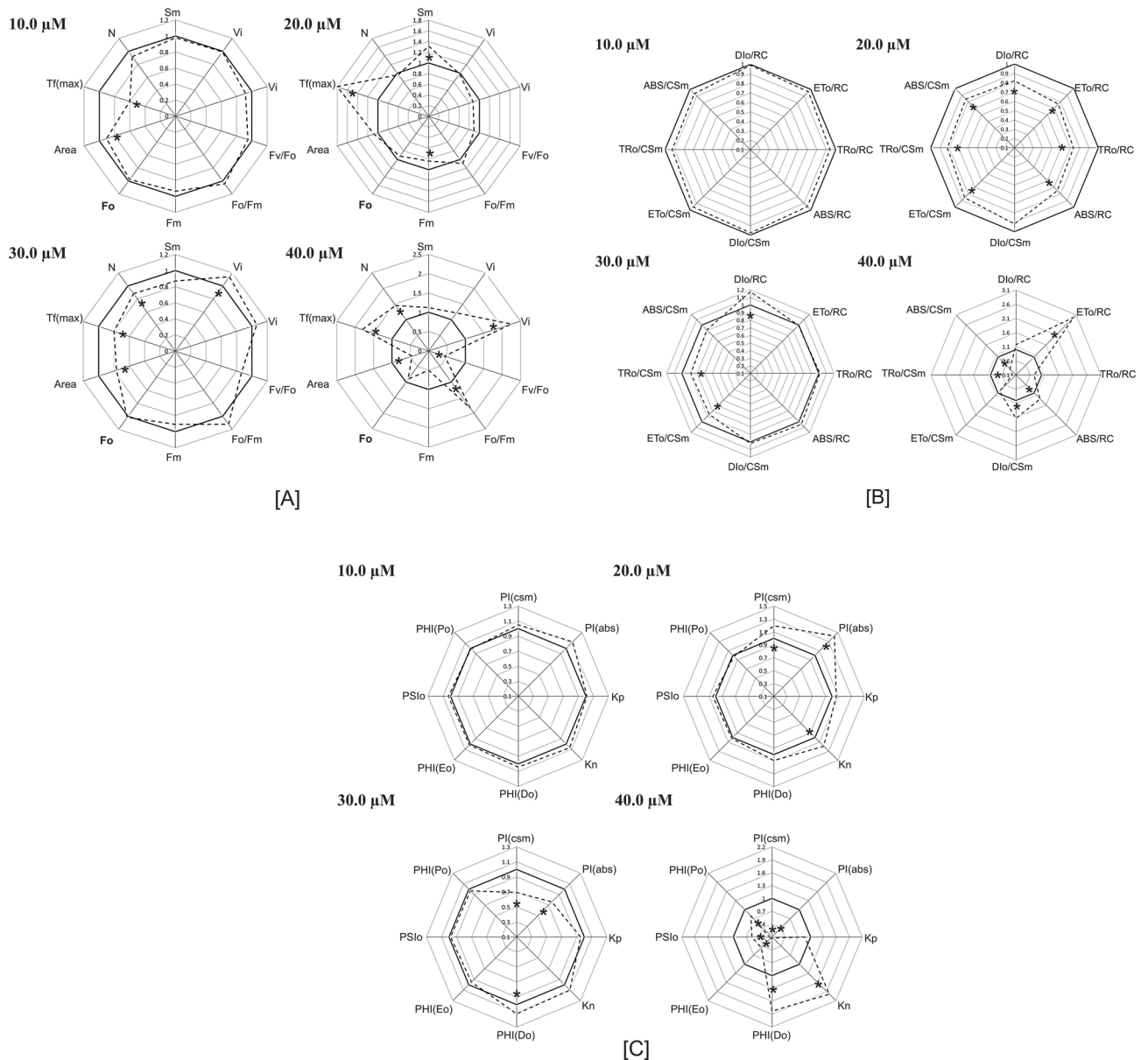
Figure 2. Radar plots (**A–C**) showing various technical fluorescence parameters. Each line represents the average of 6 measurements per treatment. Asterisk denote the significance at $p \leq 0.05$ level.

significantly declined when plants were treated with 30 μM Cu for 48 h. TR_O/CS_M reduced remarkably up to 30 μM Cu and thereafter declined up to 50% with increasing concentration of Cu (Fig. 5).

Electron transport efficiency of plants was found tolerant to Cu-induced HM stress. A high concentration of Cu (40 μM) extremely reduced the electron transfer system in thylakoid membranes (Fig. 5). DI_O/CS_M was increased significantly ($p \leq 0.05$) at 30 μM Cu treatment and after that decreased slightly).

K_P and K_N. De-excitation rate constants for nonphotochemical reaction (K_N) increased under Cu stress and at severe stress conditions K_N value approaches 198.46% of the control (Figs. 2C, 3). While de-excitation rate constants for photochemical reaction (K_P) lowered slightly (86.48% of control) at 40 μM Cu concentration.

Performance index. Overall effects of Cu-induced HM stress on various photosynthetic parameters are presented in the form of a radar plot (Fig. 2). To analyze the effects of Cu-induced HM stress on overall photosynthesis performance, PI_{ABS} and PI_{CS} were determined in *L. minor* exposed to various intensities of Cu stress. Cu stress led to a significant effect on the performance index on absorption basis (PI_{ABS}) and performance index of PS II and PS I (PI_{CS}) in *L. minor*. PI_{ABS} and PI_{CS} continuously increased with increasing concentration of Cu up to 30 μM, and then declined sharply with the progression of Cu-induced HM stress. The lowest performance index on absorption basis (PI_{ABS}) and performance index of PS II and PS I (PI_{CS}) were recorded in plants cultivated on media containing 40 μM Cu (Figs. 2C, 3).
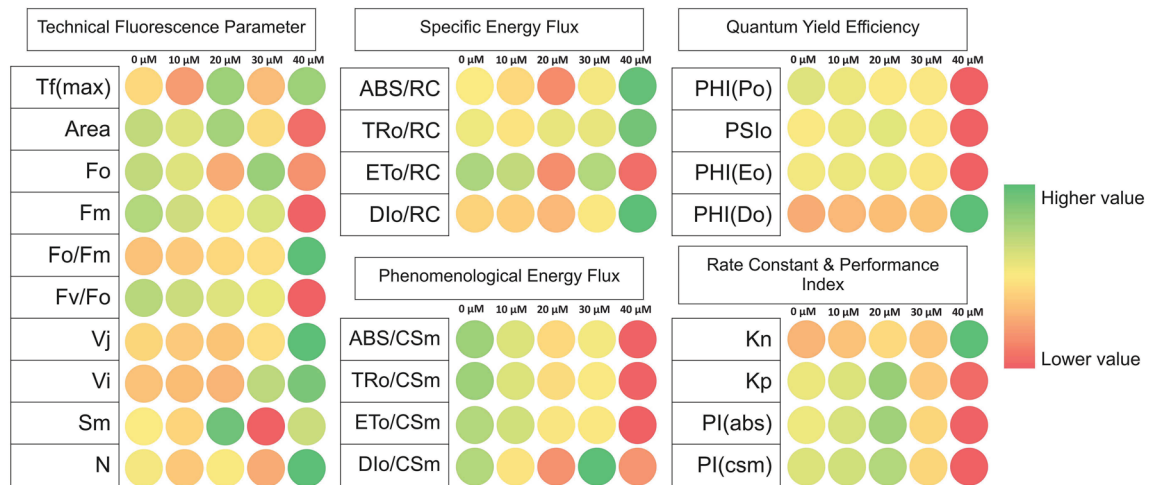
Figure 3. Heat map represents relative variability of several photosynthesis-related parameters, obtained after using the JIP test for *L. minor* under Cu stress. Data are for different concentrations (0.0 μM to 40.0 μM), obtained after 24 h red is for lower value (1%), yellow for medium (50%), and green for the highest values (100%) All the data obtained were first normalized to bring the value of the parameters in the range of 1–100 to provide an unbiased colour code.
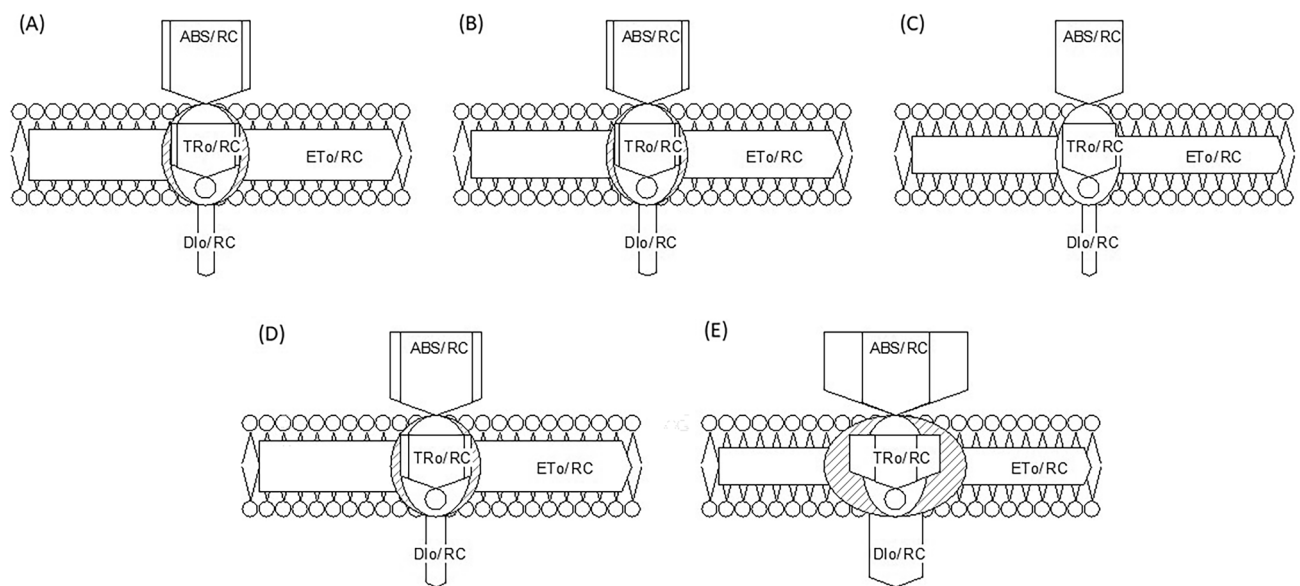

Figure 4. Thylakoid membrane model for specific energy fluxes (per reaction, RC) in *L. minor* fronds when subjected to various concentration of CuSO$_4$, (**A**); control, (**B**); 10.0 μM, (**C**); 20.0 μM, (**D**); 30.0 μM and (**E**); 40.0 μM.

The PCA results displayed that Dim 1 and Dim 2 represented 97.32% of the variation in the ChlF parameter under Cu induced HM stress in *L. minor* (Fig. 6). The loadings for ABS/CS$_O$, ET$_O$/RC, TR$_O$/CS$_O$, ET$_O$/CS$_O$, F$_V$/F$_M$, PI$_{CS}$ and PI$_{ABS}$ are in quadrate I and IV while, TR$_O$/RC, ABS/RC, DI$_O$/RC, DI$_O$/CS$_O$ and F$_O$/F$_M$ are accounted in quadrate II and III. All treatments, except 40 μM, are located in quadrate I and IV. The loading arrow of 40 μM is longer than others in all quadrates. Thus, the higher concentration of Cu was significantly affecting the major JIP parameters located in quadrate II and III. The mild Cu stress up to 20 μM was less toxic as compared to severe stress and plants performed better which was described by performance index parameters in quadrate IV (Fig. 6).

In Table 3, values of the lethal dese responsible for 50% mortality (LD$_{50}$) and 90% mortality (LD$_{90}$), calculated by probit analysis with 95% probability level, are given. The LD$_{50}$ and LD$_{90}$ values of Cu was 25.70 μM and 87.80 μM respectively.

Discussion

Many studies on the plant's physiological changes under various HM stress have been reported. These studies indicated that plants have developed a series of mechanisms to protect themselves from these adverse environmental threats. ChlF analyses have been shown to detect complex biochemical alteration in photosynthetic
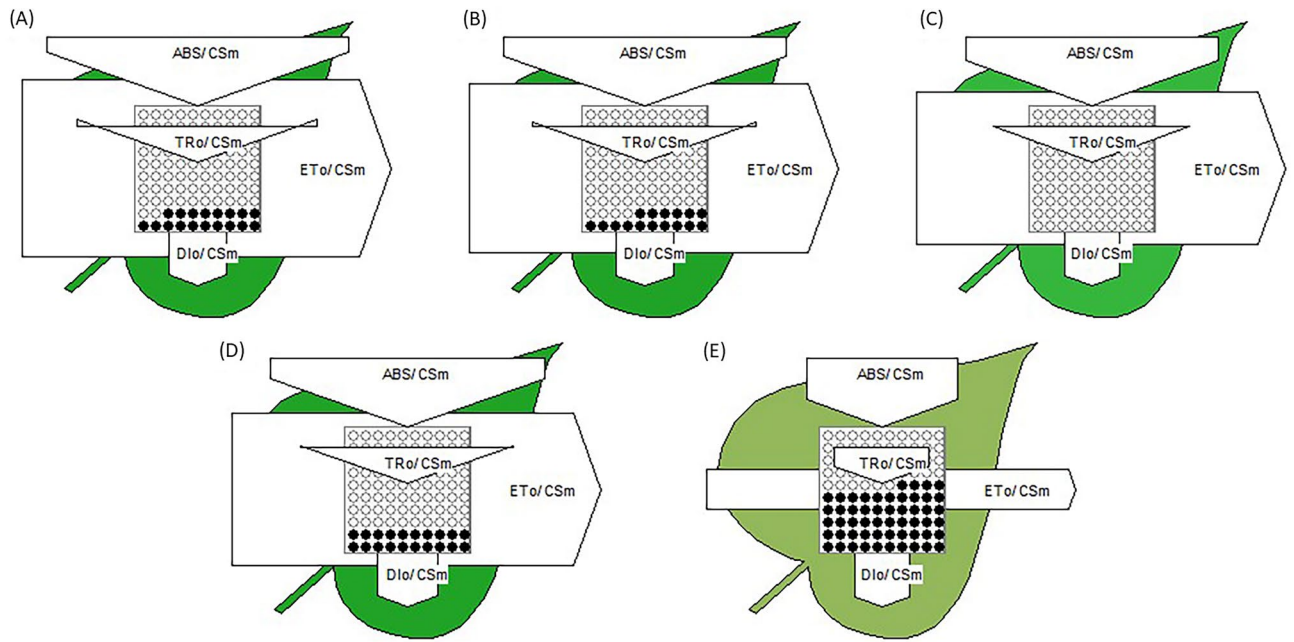
Figure 5. Energy pipeline leaf model of phenomenological fluxes (per cross section, CS) in *L. minor* fronds when subjected to various concentration of Cu, (**A**); control, (**B**); 10.0 μM, (**C**); 20.0 μM, (**D**); 30.0 μM and (**E**); 40.0 μM.
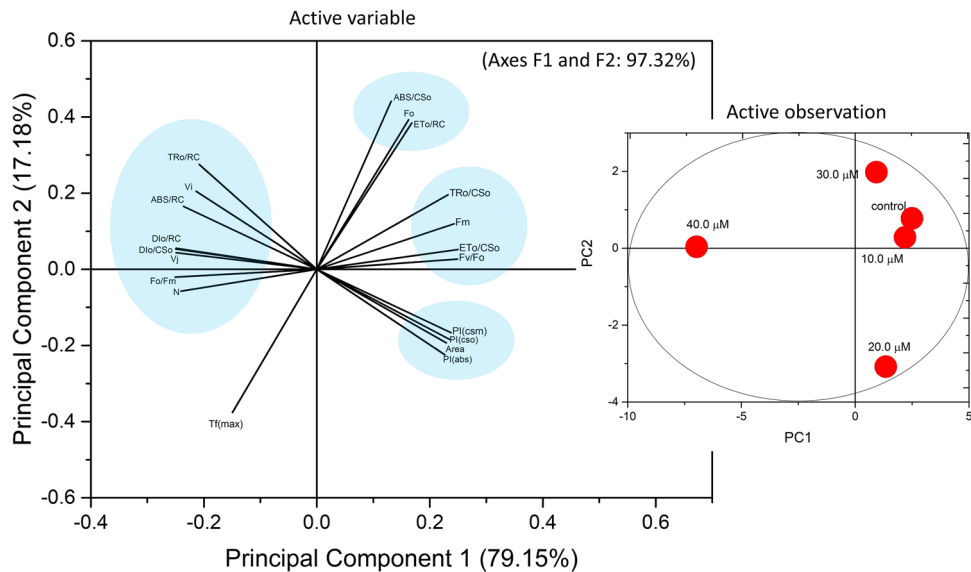

Figure 6. The principal component analysis with four Cu treatment conditions. The PCA is based on the chlorophyll fluorescence data. Arrows represent the Chlorophyll *a* fluorescence parameter on the corresponding dimensions (PC 1 and PC2), where PC 2 expressed most of the variability in the data.

apparatus in a vast range of plant species, including both terrestrial and aquatic[80]. The present investigation shows the Cu induced changes in various fluorescence parameters of photosystem II in duckweed *L. minor*.

ChlF rise. Excess energy enhanced the utilisation capacity of plants in extreme environments, after which photoprotective systems quenched the extra Chl radical, and the extra energy was dissipated as heat[79, 81, 82]. The reduction in ChlF from PSII is being used to quantify these mechanisms, which are jointly referred to as non-photochemical quenching (NPQ)[41, 83, 84]. The J-I and I-P, and the J step still appeared at the severe Cu stress (40 μM), indicating the tolerance capacity of the plant[85]. The O-J is a photochemical phase and J-I-P is a thermal phase, these are two characteristics of OJIP transient and presented three various reduction processes of the electron transport chain[52, 74, 86, 87]. The photochemical phase (O-J) is mainly light-dependent and comprises

Confidence limits							
		95% Confidence limits for Cu dose			95% Confidence limits for log(Cu dose)[a]		
	Probability	Estimate	Lower bound	Upper bound	Estimate	Lower bound	Upper bound
PROBIT	0.010	2.763	0.422	5.580	0.441	− 0.375	0.747
	0.020	3.588	0.685	6.693	0.555	− 0.165	0.826
	0.030	4.235	0.931	7.516	0.627	− 0.031	0.876
	0.040	4.798	1.172	8.204	0.681	0.069	0.914
	0.050	5.310	1.414	8.812	0.725	0.150	0.945
	0.060	5.789	1.658	9.368	0.763	0.220	0.972
	0.070	6.244	1.906	9.886	0.795	0.280	0.995
	0.080	6.682	2.159	10.376	0.825	0.334	1.016
	0.090	7.107	2.417	10.845	0.852	0.383	1.035
	0.100	7.522	2.682	11.297	0.876	0.429	1.053
	0.150	9.515	4.115	13.413	0.978	0.614	1.128
	0.200	11.469	5.756	15.441	1.060	0.760	1.189
	0.250	13.462	7.637	17.517	1.129	0.883	1.243
	0.300	15.545	9.774	19.759	1.192	0.990	1.296
	0.350	17.762	12.164	22.310	1.249	1.085	1.348
	0.400	20.158	14.767	25.378	1.304	1.169	1.404
	0.450	22.783	17.506	29.257	1.358	1.243	1.466
	0.500	25.700	20.295	34.319	1.410	1.307	1.536
	0.550	28.990	23.102	40.998	1.462	1.364	1.613
	0.600	32.765	25.971	49.837	1.515	1.414	1.698
	0.650	37.184	29.004	61.631	1.570	1.462	1.790
	0.700	42.487	32.338	77.676	1.628	1.510	1.890
	0.750	49.062	36.167	100.261	1.691	1.558	2.001
	0.800	57.588	40.792	133.789	1.760	1.611	2.126
	0.850	69.413	46.768	187.937	1.841	1.670	2.274
	0.900	87.800	55.358	289.186	1.943	1.743	2.461
	0.910	92.928	57.637	321.035	1.968	1.761	2.507
	0.920	98.838	60.211	359.670	1.995	1.780	2.556
	0.930	105.771	63.165	407.596	2.024	1.800	2.610
	0.940	114.091	66.626	468.782	2.057	1.824	2.671
	0.950	124.381	70.792	549.948	2.095	1.850	2.740
	0.960	137.663	76.006	663.573	2.139	1.881	2.822
	0.970	155.951	82.924	836.132	2.193	1.919	2.922
	0.980	184.076	93.072	1137.301	2.265	1.969	3.056
	0.990	239.053	111.575	1848.088	2.378	2.048	3.267

Table 3. The acute 48–h LD_{50} values of Cu and their confidance limits in *L. minor* according to Logit analysis. [a]Logarithm base = 10.

information regarding antenna size and connection between PSII reaction centers[88, 89]. Further, the reduction in remaining ETC is denoted by the thermal phase (J-I-P) rise[90].

Biophysical parameters derived by the 'JIP-test' equations'.
The values of minimal fluorescence intensity are an important parameter and can provide insight in the irreversible damage of PSII, associated with light-harvesting complex II (LHCII) and hindering the electron transfer on the reduced side of PSII[83, 91]. Because of conformational changes in the D1 protein under Cu stress, which cause changes in the characteristics of PSII electron acceptors, decreasing F_M under HM stress may be related to less efficient PSII activity[83].

In determining the maximum primary yield of photochemistry, F_V/F_O is a parameter that accounts for simultaneous variations in F_M and F_O[45]. The decreased values of F_V/F_O in fronds under Cu stress show the alteration in the electron transport rate to the primary electron acceptors from PSII and a reduction in the number and size of the reaction center. Martinazzo et al. and Janka et al. also reported the environmental stress-induced decrease in the F_V/F_O ratio in different plant species[92, 93]. The increased level of relative variable fluorescence under Cu treatment indicates that the electron transfer at the donor side of PSII was affected. The affected F_V/F_O can be due to the modified unquenchable fluorescence (F_O) that altered the energy relay from antenna complex to reaction center[94]. According to PCA analysis the quantum yield was positively correlated with the electron transport per cross-section while negatively correlated (Fig. 6) with F_O/F_M located in the opposite direction of the PCA loading
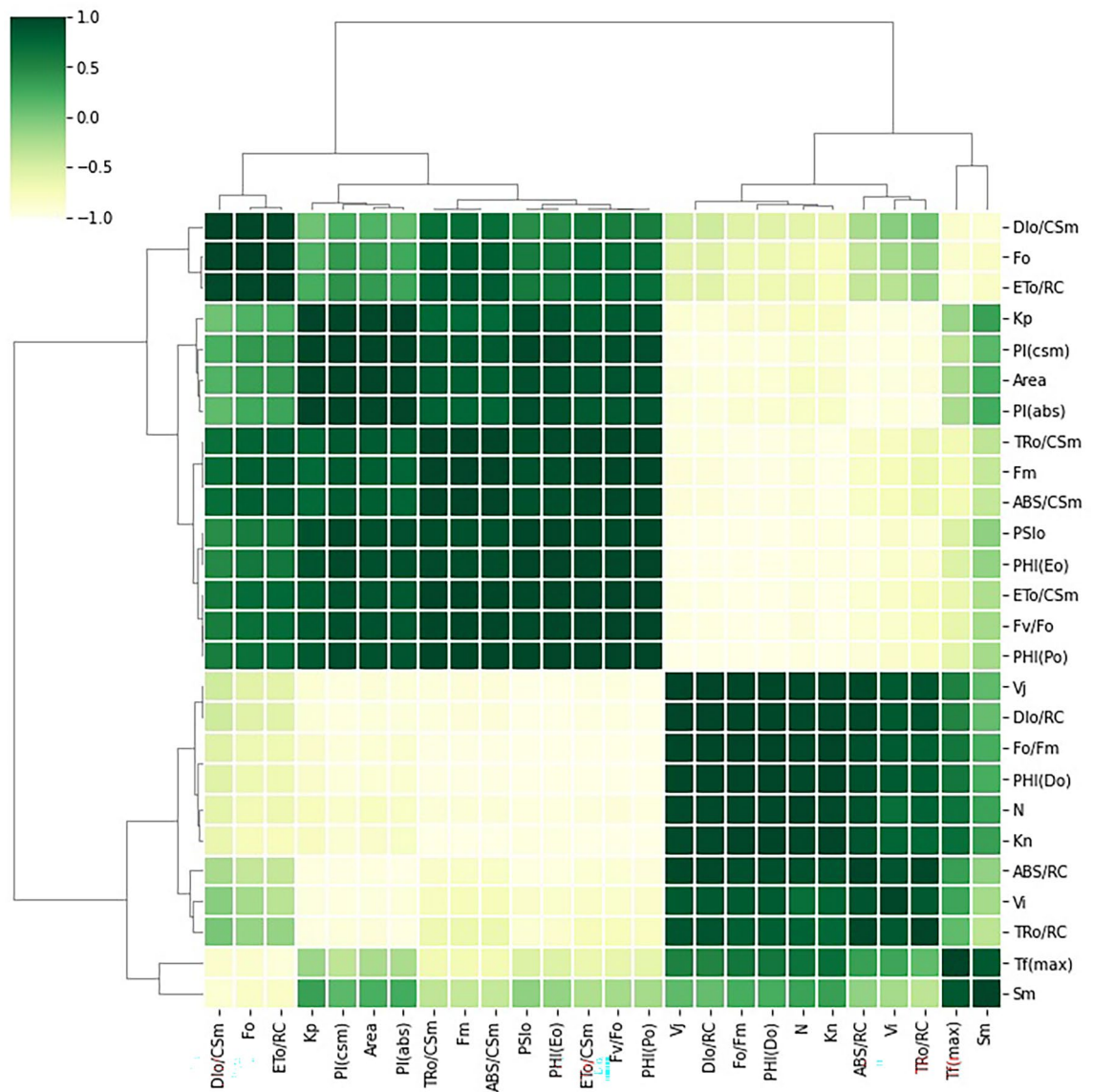
Figure 7. Grid correlation matrix shows the correlation between all calculated chlorophyll *a* fluorescence parameter with color code.

plot, which was also confirmed by the Correlation matrix (Fig. 7). Another possibility of reduced maximum primary yield under Cu stress can be the substitution of central atom of chlorophyll molecule, Mg by Cu. This substitution can hinders photosynthetic light-harvesting in the affected chlorophyll molecules[95].

The "JIP test" of fluorescence transient in photosynthetic organisms, subjected to abiotic stress revealed a marked decrease in φP_O[96]. The slight reduction in φP_O might be due to a decrease in PSII photochemical efficiency resulting from Cu stress (in most higher plants having usually a value in the range of 0.78–0.84[97]). In the light condition, a reduction in the maximum quantum yield of PSII (φPo) shows that HM stress inhibits the redox reaction following Q_A and causes a delay in electron transport between Q_A^- and Q_B.[90]. These parameters are very important and provide relevant information on electron transport activity at the PSII acceptor sites. The present finding suggested that Cu treatment reduces the electron transport at the PSII acceptor site in *L. minor*.

Energy pipeline models (membrane and leaf model), presented in Figs. 4 and 5, have displayed that various sites in PSII are sensitive to several environmental stresses[98–100]. Based on present results, TR_O/CS_M and ET_O/CS_M decreased with increasing the Cu concentration because active RCs are converted into inactive or closed (dark circle in model) RCs consequently decreasing the trapping efficiency and electron transport from PSII[74, 81, 101]. PCA biplot shown ET_O/CS_M, DI_O/CS_M are positively correlated, which is also observed by grid correlation matrix (Figs. 6, 7). The ABS/RC is determined by taking the total amount of photons absorbed by Chl molecules throughout all RCs by the total number of active RCs[58]. The ratio of active/inactive RCs influences it, and as the number of active centers rose, the ABS/RC ratio reduced. TR_O/RC is the maximum rate at which an exciton is captured by the RC, resulting in a decrease in Q_A. An increase in this ratio indicates that all the Q_A has been reduced[83]. Reduction in ET_O/RC describes that the re-oxidation of reduced Q_A through electron transport in an

active RC is decreased because a greater number of the active RC are available, hence it only reflects the activity of active RCs. Figure 4 demonstrates a reduction in per active RC electron transport but an overall increase in electron transport. The ratio of total dissipation of un-trapped excitation energy from all RCs to the number of active RCs is defined as DI_O/RC. Dissipation arises as heat, fluorescence, and energy transfer to other systems and the ratios of active/inactive RCs also have an impact. Due to the effective utilisation of energy by the active RCs, the ratio of total dissipation to the number of active RCs (DI_O/RC) is not very impacted[102, 103].

The F_V/F_M ratio = $(F_M − F_O)/F_M$ is an important JIP parameter that represents the conversion efficiency of primary light energy in the PS II reaction center and is used as a stress indicator in a large number of photosynthetic studies[53, 82, 87]. However, since it is dependent on F_O and F_M fluorescence levels, this quantitative parameter is not usually sensitive enough to detect alteration across samples. Srivastava et al. employed the performance index (PI), a novel, more responsive, and significant parameter to measure photosynthesic efficiency under stress[104]. The performance index, PI, is derived using three (or four) components based on reaction center density, trapping efficiency, and electron transport efficiency, in the same way as a Goldman equation[105]. As a result, if any of these components is affected by stress, the effect will be visible in the performance index, which has a higher sensitivity. Performance index (PI_{ABS}) is calculated on an energy absorption basis while the performance index on cross-section (PI_{CS}) is obtained by multiplying the performance index on absorption basis PI_{ABS}, by the phenomenological energy flux, $ABS/CS = Fo$ (or F_M): and the value of PIabs and P_{CS} significantly lowered in a plant grown under Cu stress (Fig. 2C). PI_{ABS} are decreased due to reduced activity of the RC so the overall activity of the RC is decreased[41, 83, 106] based on results in this study and statistical models (PCA and Correlation matrix) some of the important JIP parameters such as Phenomenological energy flux (ABS/CS_M, TR_O/CS_M and ET_O/CS_M), maximum quantum yield ($φP_O$), Performance index per absorbance (PI_{ABS}) and per cross-section (PI_{CS}) are displayed the dose–response relationship under Cu stress. Probit analysis is usually used in toxicology to determine the relative toxicity of chemicals to living organisms[107]. Copper LD50 values (Table 3) demonstrated that this molecule can be considered as highly toxic to *L. minor*. Copper phytotoxicity was assessed through the visible symptoms of toxicity and determination of the concentration that results in a 50% reduction in the growth of L. minor (LD 50). According to Teisseire & Guy (2000), CuSO4 at 10 µM was inhibitory for *L. minor* (Teisseire and Guy). However, some plant species tolerate this element at concentrations higher than those used in medium cultures. Our study indicated that, *L. minor* was sensitive to copper for concentrations ≥ 25 µM[108]. This is caused by the different duckweed species used and by the different test conditions, especially concerning the nutrient media as well as by the methods of evaluation (Appenroth et al.[109]).

Conclusion

In the present study, the efficacy of ChlF kinetics in the detection of Cu-induced HM stress was analysed in *L. minor*. Treatment of lower concentration of Cu (0.0–20.0 µM) had mild negative effect on photosynthesis. As the Cu is an essential micronutrient and plays a vital role in many biochemical processes, hence under moderate metal concentration the *L. minor* performed normally without any deleterious effect. A typical OJIP curve was obtained which shows that the plant efficiently used the solar energy for photosynthesis which is expressed in the term of increased active reaction center and performance index. In contrast, at higher Cu concentration (30.0–40.0 µM), the OJIP curve has been flattened due to a reduction in electron transport towards PSI (P_{700}), and a major portion of absorbed energy was dissipated in the form of heat because of an increased number of the inactive reaction center. Conclusively, phenomenological energy flux (ABS/CS_M, TR_O/CS_M and ET_O/CS_M), maximum quantum yield ($φP_O$), performance indexes (PI_{ABS} and PI_{CS}) are powerful indicators of HM stress in plants and can be used for rapid detection of HM-induced water pollutant.Additionally, the key OJIP parameters screened in this paper could be a good tool for the rapid detaction of primary mode of action of HM on the photosynthetic apparatus in *L. minor*.

Data availability

The datasets used and/or analysed during the current study available from the corresponding author on reasonable request.

References

1. Aydinalp, C. & Marinova, S. The effects of heavy metals on seed germination and plant growth on alfalfa plant (*Medicago sativa*). *Bulg. J. Agric. Sci.* **15**, 347–350 (2009).
2. Öztürk, M. A. *Plants and Pollutants in Developed and Developing Countries* (Ege University, 1989).
3. Ali, I. & Jain, C. K. Advances in arsenic speciation techniques. *Int. J. Environ. Anal. Chem.* **84**, 947–964 (2004).
4. Krzesłowska, M. The cell wall in plant cell response to trace metals: Polysaccharide remodeling and its role in defense strategy. *Acta Physiol. Plant.* **33**, 35–51 (2011).
5. Ali, I., Gupta, V. K., Khan, T. A. & Asim, M. Removal of arsenate from aqueous solution by electro-coagulation method using Al-Fe electrodes. *Int. J. Electrochem. Sci.* **7**, 1898–1907 (2012).
6. Ali, I., ALOthman, Z. A. & Sanagi, M. M. Green synthesis of iron nano-impregnated adsorbent for fast removal of fluoride from water. *J. Mol. Liq.* **211**, 457–465 (2015).
7. Suhail, M. & Ali, I. Advanced spiral periodic classification of the elements. *Chem. Int.* **3**, 220–224 (2017).
8. Ali, I. *et al.* Artificial neural network modelling of amido black dye sorption on iron composite nano material: Kinetics and thermodynamics studies. *J. Mol. Liq.* **250**, 1–8 (2018).
9. Sabir, M. *et al.* Phytoremediation: Mechanisms and adaptations. *Soil Remediat. Plants Prospect. Challenges* **85**, 85–105 (2014).
10. Dehghani, M. H., Sanaei, D., Ali, I. & Bhatnagar, A. Removal of chromium (VI) from aqueous solution using treated waste newspaper as a low-cost adsorbent: Kinetic modeling and isotherm studies. *J. Mol. Liq.* **215**, 671–679 (2016).
11. Alharbi, O. M. L. *et al.* Health and environmental effects of persistent organic pollutants. *J. Mol. Liq.* **263**, 442–453 (2018).

12. Basheer, A. A. New generation nano-adsorbents for the removal of emerging contaminants in water. *J. Mol. Liq.* **261**, 583–593 (2018).

13. Burakova, E. A. *et al.* Novel and economic method of carbon nanotubes synthesis on a nickel magnesium oxide catalyst using microwave radiation. *J. Mol. Liq.* **253**, 340–346 (2018).

14. Gough, L. P. *Element Concentrations Toxic to Plants, Animals and Man* (1979).

15. Adriano, D. C. *Trace Elements in the Terrestrial Environment* (Springer, 2013).

16. Guecel, S. *et al.* Studies on trace metals in soils and plants growing in the vicinity of copper mining area-Lefke, Cyprus. *Fresenius Environ. Bull.* **18**, 360–368 (2009).

17. Ashraf, M., Ozturk, M. & Ahmad, M. S. A. Toxins and their phytoremediation. In *Plant Adaptation and Phytoremediation* (eds Ashraf, M. *et al.*) 1–32 (Springer, 2010).

18. Sharma, S. *et al.* Adsorption of Rhodamine B dye from aqueous solution onto acid activated mango (*Magnifera indica*) leaf powder: Equilibrium, kinetic and thermodynamic studies. *J. Toxicol. Environ. Health Sci.* **3**, 286–297 (2011).

19. Ozturk, M. & Turkan, I. Heavy metal accumulation by plants growing alongside the motor roads: A case study from Turkey. In *Plants as Biomonitors Indic. Heavy Met. Terr. Environ.* 515–522 (1993).

20. Aksoy, A. & Öztürk, M. A. *Phoenix dactylifera L. as a Biomonitor of Heavy Metal Pollution in Turkey* (1996).

21. Ali, I. & Aboul-Enein, H. Y. Speciation of arsenic and chromium metal ions by reversed phase high performance liquid chromatography. *Chemosphere* **48**, 275–278 (2002).

22. Mukherjee, A., Agrawal, S. B. & Agrawal, M. Heavy metal accumulation potential and tolerance in tree and grass species. In *Plant Responses to Xenobiotics* (eds Singh, A. *et al.*) 177–210 (Springer, 2016).

23. Ashraf, S., Ali, Q., Zahir, Z. A., Ashraf, S. & Asghar, H. N. Phytoremediation: Environmentally sustainable way for reclamation of heavy metal polluted soils. *Ecotoxicol. Environ. Saf.* **174**, 714–727 (2019).

24. Öztürk, M., Özözen, G., Minareci, O. & Minareci, E. Determination of heavy metals in of fishes, water and sediment from the Demirköprü Dam Lake (Turkey). *J. Appl. Biol. Sci.* **2**, 99–104 (2008).

25. Singh, H., Kumar, D. & Soni, V. Copper and mercury induced oxidative stresses and antioxidant responses of *Spirodela polyrhiza* (L.) Schleid. *Biochem. Biophys. Rep.* **23**, 100781 (2020).

26. Raj, S., Singh, H., Trivedi, R. & Soni, V. Biogenic synthesis of AgNPs employing *Terminalia arjuna* leaf extract and its efficacy towards catalytic degradation of organic dyes. *Sci. Rep.* **10**, 9616 (2020).

27. Bouazizi, H., Jouili, H., Geitmann, A. & El Ferjani, E. Copper toxicity in expanding leaves of *Phaseolus vulgaris* L.: Antioxidant enzyme response and nutrient element uptake. *Ecotoxicol. Environ. Saf.* **73**, 1304–1308 (2010).

28. Yadav, S. K. Heavy metals toxicity in plants: An overview on the role of glutathione and phytochelatins in heavy metal stress tolerance of plants. *S. Afr. J. Bot.* https://doi.org/10.1016/j.sajb.2009.10.007 (2010).

29. Neelima, P. & Reddy, K. J. Interaction of copper and cadmium with seedling growth and biochemical responses in *Solanum melongena*. *Nat. Environ. Pollut. Technol.* **1**, 285–290 (2002).

30. Percival, G. C., Keary, I. P. & Sulaiman, A.-H. An assessment of the drought tolerance of Fraxinus genotypes for urban landscape plantings. *Urban For. Urban Green.* **5**, 17–27 (2006).

31. Binder, W. D. & Fielder, P. Chlorophyll fluorescence as an indicator of frost hardiness in white spruce seedlings from different latitudes. *New For.* **11**, 233–253 (1996).

32. Maxwell, K. & Johnson, G. N. Chlorophyll fluorescence—A practical guide. *J. Exp. Bot.* **51**, 659–668 (2000).

33. Hermans, C. *et al.* Quality assessment of urban trees: A comparative study of physiological characterisation, airborne imaging and on site fluorescence monitoring by the OJIP-test. *J. Plant Physiol.* **160**, 81–90 (2003).

34. Papageorgiou, G. C. *et al.* Eugene I. Rabinowitch: A prophet of photosynthesis and of peace in the world. *Photosynth. Res.* **141**, 143–150 (2019).

35. Baker, N. R. & Rosenqvist, E. Applications of chlorophyll fluorescence can improve crop production strategies: An examination of future possibilities. *J. Exp. Bot.* **55**, 1607–1621 (2004).

36. L'Hirondelle, S. J., Simpson, D. G. & Binder, W. D. Chlorophyll fluorescence, root growth potential, and stomatal conductance as estimates of field performance potential in conifer seedlings. *New For.* **34**, 235–251 (2007).

37. Murchie, E. H. & Lawson, T. Chlorophyll fluorescence analysis: A guide to good practice and understanding some new applications. *J. Exp. Bot.* **64**, 3983–3998 (2013).

38. Salvatori, E. *et al.* Plant stress analysis: Application of prompt, delayed chlorophyll fluorescence and 820 nm modulated reflectance. Insights from independent experiments. *Plant Physiol. Biochem.* **85**, 105–113 (2014).

39. Pollastrini, M. *et al.* Taxonomic and ecological relevance of the chlorophyll a fluorescence signature of tree species in mixed European forests. *New Phytol.* **212**, 51–65 (2016).

40. Fusaro, L., Salvatori, E., Mereu, S. & Manes, F. Photosynthetic traits as indicators for phenotyping urban and peri-urban forests: A case study in the metropolitan city of Rome. *Ecol. Indic.* **103**, 301–311 (2019).

41. Kumar, D., Singh, H., Raj, S. & Soni, V. Chlorophyll a fluorescence kinetics of mung bean (*Vigna radiata* L.) grown under artificial continuous light. *Biochem. Biophys. Reports* **24**, 100813 (2020).

42. Stirbet, A. & Govindjee,. On the relation between the Kautsky effect (chlorophyll a fluorescence induction) and Photosystem II: Basics and applications of the OJIP fluorescence transient. *J. Photochem. Photobiol. B Biol.* **104**, 236. https://doi.org/10.1016/j.jphotobiol.2010.12.010 (2011).

43. Pogrzeba, M. *et al.* Relationships between soil parameters and physiological status of *Miscanthus* x *giganteus* cultivated on soil contaminated with trace elements under NPK fertilisation vs. microbial inoculation. *Environ. Pollut.* **225**, 163–174 (2017).

44. Singh, H. *et al.* Tolerance and decolorization potential of duckweed (*Lemna gibba*) to C.I. Basic Green 4. *Sci. Rep.* **11**, 10889 (2021).

45. Tuba, Z. *et al.* Chlorophyll a fluorescence measurements for validating the tolerant bryophytes for heavy metal (Pb) biomapping. *Curr. Sci.* **98**, 1505–1508 (2010).

46. Kumar, D., Singh, H., Bhatt, U., Soni, V. & Allakhverdiev, S. Effect of continuous light on antioxidant activity, lipid peroxidation, proline and chlorophyll content in *Vigna radiata* L.. *Funct. Plant Biol.* **49**, 145 (2021).

47. Baker, N. R. & Oxborough, K. Chlorophyll fluorescence as a probe of photosynthetic productivity. In *Chlorophyll a Fluorescence* (eds Papageorgiou, G. C. & Govindjee) 65–82 (Springer, 2004).

48. Stirbet, A. *et al.* Chlorophyll a fluorescence induction in higher plants: Modelling and numerical simulation. *J. Theor. Biol.* **193**, 131–151 (1998).

49. Dietz, K.-J. & Pfannschmidt, T. Novel regulators in photosynthetic redox control of plant metabolism and gene expression. *Plant Physiol.* **155**, 1477–1485 (2011).

50. Hall, J. L. Cellular mechanisms for heavy metal detoxification and tolerance. *J. Exp. Bot.* https://doi.org/10.1093/jxb/53.366.1 (2002).

51. Sharma, S. S. & Dietz, K. J. The relationship between metal toxicity and cellular redox imbalance. *Trends Plant Sci.* **14**, 43–50 (2009).

52. Stirbet, A. & Govindjee,. Chlorophyll a fluorescence induction: A personal perspective of the thermal phase, the J-I-P rise. *Photosynth. Res.* **113**, 15–61 (2012).

53. Kalaji, H. M. *et al.* Experimental in vivo measurements of light emission in plants: A perspective dedicated to David Walker. *Photosynth. Res.* **114**, 69–96 (2012).

54. Schansker, G., Tóth, S. Z., Holzwarth, A. R. & Garab, G. Chlorophyll a fluorescence: Beyond the limits of the QA model. *Photosynth. Res.* **120**, 43–58 (2014).
55. Dkabrowski, P., Pawluśkiewicz, B., Baczewska, A. H. & Oglkecki Pawełand Kalaji, H. Chlorophyll a fluorescence of perennial ryegrass (*Lolium perenne* L.) varieties under long term exposure to shade. *Zemdirbyste-Agriculture* **102**, 305 (2015).
56. Živčák, M. *et al.* Measurements of chlorophyll fluorescence in different leaf positions may detect nitrogen deficiency in wheat. *Zemdirbyste-Agriculture* **101**, 437 (2014).
57. Kalaji, H. & Nalborczyk, E. Gas exchange of barley seedlings growing under salinity stress. *Photosynthesis* **25**, 197–202 (1991).
58. Rapacz, M., Sasal, M., Kalaji, H. M. & Kościelniak, J. Is the OJIP test a reliable indicator of winter hardiness and freezing tolerance of common wheat and triticale under variable winter environments? *PLoS ONE* **10**, e0134820 (2015).
59. Dkabrowski, P. *et al.* Delayed chlorophyll a fluorescence, MR 820, and gas exchange changes in perennial ryegrass under salt stress. *J. Lumin.* **183**, 322–333 (2017).
60. Baker, A. J. M. & Brooks, R. Terrestrial higher plants which hyperaccumulate metallic elements. A review of their distribution, ecology and phytochemistry. *Biorecovery* **1**, 81–126 (1989).
61. Dan, T. V., KrishnaRaj, S. & Saxena, P. K. Metal tolerance of scented geranium (*Pelargonium* sp. 'Frensham'): Effects of cadmium and nickel on chlorophyll fluorescence kinetics. *Int. J. Phytoremediat.* **2**, 91–104 (2000).
62. Bolhar-Nordenkampf, H. R. *et al.* Chlorophyll fluorescence as a probe of the photosynthetic competence of leaves in the field: A review of current instrumentation. *Funct. Ecol.* **3**, 497–514 (1989).
63. KrishnaRaj, S., Mawson, B. T., Yeung, E. C. & Thorpe, T. A. Utilization of induction and quenching kinetics of chlorophyll a fluorescence for in vivo salinity screening studies in wheat (*Triticum aestivum* vars. Kharchia-65 and Fielder). *Can. J. Bot.* **71**, 87–92 (1993).
64. Devlamynck, R. *et al. Lemna minor* cultivation for treating swine manure and providing micronutrients for animal feed. *Plants* **10**, 1124 (2021).
65. Dewez, D., Goltsev, V., Kalaji, H. M. & Oukarroum, A. Inhibitory effects of silver nanoparticles on photosystem II performance in *Lemna gibba* probed by chlorophyll fluorescence. *Curr. Plant Biol.* **16**, 15–21 (2018).
66. Whitacre, D. M. *Reviews of Environmental Contamination and Toxicology* Vol. 232 (Springer, 2014).
67. National Biodiversity Authority. *National Biodiversity Act, 2002* (MOEF, 2002).
68. OECD. Lemna sp. Growth Inhibition Test. *Oecd Guidel. Test. Chem.* 22 (2002).
69. Dirilgen, N. Mercury and lead: Assessing the toxic effects on growth and metal accumulation by *Lemna minor*. *Ecotoxicol. Environ. Saf.* **74**, 48–54 (2011).
70. Teisseire, H. & Guy, V. Copper-induced changes in antioxidant enzymes activities in fronds of duckweed (*Lemna minor*). *Plant Sci.* https://doi.org/10.1016/S0168-9452(99)00257-5 (2000).
71. Strasser, R. J., Tsimilli-Michael, M. & Srivastava, A. Analysis of the chlorophyll a fluorescence transient. In *Chlorophyll a Fluorescence* (eds Papageorgiou, G. C. & Govindjee) 321–362 (Springer, 2004).
72. Strasser, R. G. On the OJIP fluorescence transient in leaves and D1 mutants of *Chlamydomonas reinhardtii*. In *Research in Photosynthesis: Proceedings of the IXth International Congress on Photosynthesis*, Vol. 2, 29–32 (1992).
73. Strasser, R. J., Srivastava, A. & Tsimilli-Michael, M. *The Fluorescence Transient as a Tool to Characterize and Screen Photosynthetic Samples. Probing Photosynthesis: Mechanisms, Regulation and Adaptation* (2000).
74. Strasser, R. J., Srivastava, A. & Govindjee,. Polyphasic chlorophyll a fluorescence transient in plants and cyanobacteria. *Photochem. Photobiol.* **61**, 32–42 (1995).
75. Stirbet, A. Biology On the relation between the Kautsky effect (chlorophyll a fluorescence induction) and Photosystem II: Basics and applications of the OJIP fluorescence transient q. *J. Photochem. Photobiol. B Biol.* **104**, 236–257 (2011).
76. Bhatt, U. *et al.* Rehydration quickly assembles photosynthetic complexes in desiccation tolerant *Riccia gangetica*. *Biomed. J. Sci. Tech. Res.* **30**, 23034–23037 (2020).
77. Bhatt, U., Singh, H., Kumar, D. & Soni, V. Rehydration induces quick recovery of photosynthesis in desiccation tolerant moss *Semibarbula orientalis*. *J. Plant Sci. Res.* **35**, 183 (2019).
78. Bhatt, U., Singh, H., Kumar, D., Strasser, R. J. & Soni, V. Severe leaf-vein infestation upregulates antioxidant and photosynthetic activities in the lamina of *Ficus religiosa*. *Acta Physiol. Plant* **44**, 1–9 (2022).
79. Soni, V., Keswani, K., Bhatt, U., Kumar, D. & Singh, H. In vitro propagation and analysis of mixotrophic potential to improve survival rate of *Dolichandra unguis*-cati under ex vitro conditions. *Heliyon* **7**, e06101 (2021).
80. Gonzalez-Mendoza, D. *et al.* Copper stress on photosynthesis of black mangle (*Avicennia germinans*). *An. Acad. Bras. Cienc.* **85**, 665–670 (2013).
81. Tsimilli-Michael, M. Revisiting JIP-test: An educative review on concepts, assumptions, approximations, definitions and terminology. *Photosynthetica* **58**, 275–292 (2020).
82. Baker, N. Chlorophyll fluorescence: A probe of photosynthesis in vivo. *Annu. Rev. Plant Biol.* **59**, 89–113 (2008).
83. Kalaji, H. M. *et al.* Frequently asked questions about in vivo chlorophyll fluorescence: Practical issues. *Photosynth. Res.* https://doi.org/10.1007/s11120-014-0024-6 (2014).
84. Kalaji, H. M. *et al.* Chlorophyll a fluorescence as a tool to monitor physiological status of plants under abiotic stress conditions. *Acta Physiol. Plant* **38**, 102 (2016).
85. Panda, D., Rao, D. N., Sharma, S. G., Strasser, R. J. & Sarkar, R. K. Submergence effects on rice genotypes during seedling stage: Probing of submergence driven changes of photosystem 2 by chlorophyll a fluorescence induction OJIP transients. *Photosynthetica* **44**, 69–75 (2006).
86. Schansker, G. *et al.* Characterization of the 820-nm transmission signal paralleling the chlorophyll a fluorescence rise (OJIP) in pea leaves. *Funct. Plant Biol.* **30**, 785–796 (2003).
87. Strasser, R. J., Tsimilli-Michael, M. & Srivastava, A. Analysis of the chlorophyll a fluorescence transient. In *Chlorophyll a Fluorescence: A Signature of Photosynthesis* (eds Papageorgiou, G. C. & Govindjee) 321–362 (Springer, 2004).
88. Neubauer, C. & Schreiber, U. The polyphasic rise of chlorophyll fluorescence upon onset of strong continuous illumination: I. Saturation characteristics and partial control by the photosystem II acceptor side. *Z. für Nat. C* **42**, 1246–1254 (1987).
89. Schansker, G., Tóth, S. Z. & Strasser, R. J. Dark recovery of the Chl a fluorescence transient (OJIP) after light adaptation: The qT-component of non-photochemical quenching is related to an activated photosystem I acceptor side. *Biochim. Biophys. Acta Bioenerg.* **1757**, 787–797 (2006).
90. Schansker, G., Tóth, S. Z. & Strasser, R. J. Methylviologen and dibromothymoquinone treatments of pea leaves reveal the role of photosystem I in the Chl a fluorescence rise OJIP. *Biochim. Biophys. Acta Bioenerg.* **1706**, 250–261 (2005).
91. Goltsev, V. N. *et al.* Variable chlorophyll fluorescence and its use for assessing physiological condition of plant photosynthetic apparatus. *Russ. J. Plant Physiol.* https://doi.org/10.1134/S1021443716050058 (2016).
92. Martinazzo, E. G., Ramm, A. & Bacarin, M. A. The chlorophyll a fluorescence as an indicator of the temperature stress in the leaves of *Prunus persica*. *Braz. J. Plant Physiol.* https://doi.org/10.1590/S1677-04202013005000001 (2012).
93. Janka, E., Körner, O., Rosenqvist, E. & Ottosen, C. O. High temperature stress monitoring and detection using chlorophyll a fluorescence and infrared thermography in chrysanthemum (*Dendranthema grandiflora*). *Plant Physiol. Biochem.* https://doi.org/10.1016/j.plaphy.2013.02.025 (2013).
94. DeEll, J. R., Kooten, O. V., Prange, R. K. & Murr, D. P. Applications of chlorophyll fluorescence techniques in postharvest physiology. *Hortic. Rev. (Am. Soc. Hortic. Sci.)* **23**, 69–107 (2010).

95. Küpper, H., Šetlík, I., Spiller, M., Küpper, F. C. & Prášil, O. Heavy metal-induced inhibition of photosynthesis: Targets of in vivo heavy metal chlorophyll formation. *J. Phycol.* **38**, 429–441 (2002).
96. Tsimilli-Michael, M., Pêcheux, M. & Strasser, R. J. Vitality and stress adaptation of the symbionts of coral reef and temperate foraminifers probed in hospite by the fluorescence kinetics OJIP. *Arch. Des. Sci.* **51**, 205–240 (1998).
97. Björkman, O. & Demmig, B. Photon yield of O 2 evolution and chlorophyll fluorescence characteristics at 77 K among vascular plants of diverse origins. *Planta* **170**, 489–504 (1987).
98. Gautam, A., Agrawal, D., SaiPrasad, S. V. & Jajoo, A. A quick method to screen high and low yielding wheat cultivars exposed to high temperature. *Physiol. Mol. Biol. Plants* **20**, 533–537 (2014).
99. Mehta, P., Jajoo, A., Mathur, S. & Bharti, S. Chlorophyll a fluorescence study revealing effects of high salt stress on Photosystem II in wheat leaves. *Plant Physiol. Biochem.* **48**, 16–20 (2010).
100. Zushi, K., Kajiwara, S. & Matsuzoe, N. Chlorophyll a fluorescence OJIP transient as a tool to characterize and evaluate response to heat and chilling stress in tomato leaf and fruit. *Sci. Hortic. (Amsterdam)* **148**, 39–46 (2012).
101. Zushi, K. & Matsuzoe, N. Using of chlorophyll a fluorescence OJIP transients for sensing salt stress in the leaves and fruits of tomato. *Sci. Hortic. (Amsterdam)* **219**, 216–221 (2017).
102. Grieco, M., Suorsa, M., Jajoo, A., Tikkanen, M. & Aro, E. M. Light-harvesting II antenna trimers connect energetically the entire photosynthetic machinery—Including both photosystems II and I. *Biochim. Biophys. Acta Bioenerg.* https://doi.org/10.1016/j.bbabio.2015.03.004 (2015).
103. Heber, U., Soni, V. & Strasser, R. J. Photoprotection of reaction centers: Thermal dissipation of absorbed light energy vs charge separation in lichens. *Physiol. Plant.* **142**, 65–78 (2011).
104. Srivastava, A. *et al.* Greening of peas: Parallel measurements of 77 K emission spectra, OJIP chlorophyll a fluorescence transient, period four oscillation of the initial fluorescence level, delayed light emission, and P700. *Photosynthetica* **37**, 365–392 (1999).
105. Goldman, D. E. Potential, impedance, and rectification in membranes. *J. Gen. Physiol.* **27**, 37–60 (1943).
106. Kalaji, H. M. *et al.* Frequently asked questions about chlorophyll fluorescence, the sequel. *Photosynth. Res.* **132**, 13–66 (2017).
107. Hassan, J. & Tabarraei, H. Toxicity of copper on rainbow trout: Lethal concentration or lethal dose evaluation. *Environ. Sci* **11**, 98–102 (2015).
108. Kellaf, N. & Zardoui, M. Growth, photosynthesis and respiratory response to copper in Lemna minor: A potential use of duckweed in biomonitoring. *J. Environ. Health Sci. Eng.* **7**, 299–306 (2010).
109. Appenroth, K.-J., Krech, K., Keresztes, A., Fischer, W. & Koloczek, H. Effects of nickel on the chloroplasts of the duckweeds *Spirodela polyrhiza* and *Lemna minor* and their possible use in biomonitoring and phytoremediation. *Chemosphere* **78**, 216–223 (2010).
110. Stirbet, A. & Govindjee,. Chlorophyll a fluorescence induction: Understanding the thermal phase, the JIP rise. *Photosyn. Res* **113**, 15–61 (2012).

Acknowledgements

Author contributions

H.S. conceived the original screening and research plans; V.S. supervised the experiments; H.S.; D.K. and V.S. performed the experiments; H.S. designed the experiments and analyzed the data; H.S. conceived the project and wrote the article with contributions of all the authors; V.S. supervised and completed the writing and agrees to serve as the author responsible for contact and ensures communication.

Competing interests

The authors declare no competing interests.

Additional information

Correspondence and requests for materials should be addressed to V.S.

Reprints and permissions information is available at www.nature.com/reprints.

Publisher's note Springer Nature remains neutral with regard to jurisdictional claims in published maps and institutional affiliations.